Polymer Vol. 39 No. 25, pp. 6611–6620, 1998

0032-3861/98/$ - see front matter

PII: S0032-3861(98)00167-0

Characterization of ultra-high molar mass hyaluronan: 1. Off-line static methods

Raniero Mendichi[a,*], Alberto Giacometti Schieroni[a], Cesare Grassi[b] and Alberto Re[b]

[a]*Istituto di Chimica delle Macromolecole (CNR), Via Bassini 15, 20133 Milan, Italy*
[b]*Pharmacia and Upjohn, Viale Pasteur 10, 20014 Nerviano (MI), Italy*
(Revised 18 February 1998)

This study concerns the problems encountered in the molecular characterization of ultra-high molar mass (UHMM) hyaluronan samples. The determination of the molar mass distribution of UHMM polymers is fairly difficult. Shear degradation and non-newtonian flow are the main difficulties in the fractionation on SEC columns. Considering these difficulties, the samples have remained previously characterized by off-line light scattering and viscometry. The characterization by means of light scattering presents the problem of non linear angular variation of the scattering. We present a method to estimate reliable values for molar mass and dimensions of UHMM hyaluronan polymers. To overcome the intrinsic viscosity shear rate dependence we have used a multi-bulb capillary viscometer. The persistence length of the UHMM hyaluronan polymer has been estimated. © 1998 Elsevier Science Ltd. All rights reserved.

(Keywords: hyaluronan; ultra-high molar mass; multi-angle light scattering)

INTRODUCTION

Hyaluronan (HA) is a polysaccharide of relevant interest. The origins of HA are both extractive, from varied sources, and fermentative (biotechnology). HA in aqueous solution is not neutral, but is a negatively charged polyelectrolyte. The molar mass of the HA polymers ranges from relatively low to high and ultra-high values (up to 1×10^7 g mol^{-1}). This study concerns the problems encountered in the molecular characterization of ultra-high molar mass (UHMM) HA samples with molar mass ranging from 1×10^6 to 1×10^7 g mol^{-1}. The determination of the true molar mass distribution (MMD) of UHMM polymers is fairly difficult. Every time size exclusion chromatography (SEC) fractionation was applied to UHMM polymers, severe problems were invariably reported. The main problems were shear degradation, concentration effects, poor columns resolution and, in general, low reproducibility[1,2]. Therefore, considering the difficulties met in the fractionation of UHMM HA polymers, particularly the risk of degradation in the columns, the samples were previously characterized by the static off-line mode. Our goal was to obtain reliable values of molar mass, dimension and intrinsic viscosity of the UHMM HA samples. The results obtained by off-line LS and by off-line viscometry will be used as reference for the on-line SEC results. This paper reports only the off-line LS and viscometry results. A following paper will report the results obtained by the on-line SEC characterization.

EXPERIMENTAL

Materials

Several UHMM HA samples, from different sources, were obtained from Pharmacia & Upjohn (Nerviano (MI), Italy). Seven samples were from an extractive source, cock's comb, with molar mass ranging from 1×10^6 to 7×10^6 g mol^{-1}. Other samples were from a fermentative source with molar mass ranging from 4×10^6 to 1×10^7 g mol^{-1}. All the samples were highly purified hyaluronan, typically containing less than 0.2% protein. Bovine serum albumin (BSA) was obtained from Sigma (USA). All chemicals were of analytical grade. Water solvent was Milli-Q grade (Millipore, MA, USA).

Methods

Light scattering. Samples were characterized in 0.15 M NaCl solvent at 25°C by means of a multi-angle light scattering (MALS) photometer Dawn DSP-F from Wyatt (S. Barbara CA, USA). Some samples were also characterized in higher ionic strength solvent: 0.5 M NaCl. The MALS instrument, with a vertically polarized laser of wavelength 632.8 nm, measures the intensity of the scattered light at 18 fixed angular locations ranging in the solvent, K5 flow cell, from 14.5° to 158.3°. The calibration constant was calculated using toluene as a standard assuming a rayleigh factor (R_θ) value of 1.406×10^{-5} cm^{-1}. The photodiodes normalization was carried out by measuring the scattering intensity in the solvent of a BSA globular protein assumed to act as an isotropic scatterer. All the HA solutions used in the LS measurements were exhaustively dialysed against the proper solvent. Data acquisition and analysis software was Dawn 3.01 from Wyatt. Details of the MALS instrument, hardware and software, have been described elsewhere[3]. For comparison, the molar mass of some samples has also measured by means of a low-angle light scattering (LALS) photometer KMX-6 from LDC Milton Roy (USA).

The specific refractive index increment, dn/dc, was determined by means of a KMX-16, LDC Milton Roy, differential refractometer. The differences of the dn/dc values in 0.15 M NaCl and in 0.5 M NaCl solvents for HA

* To whom correspondence should be addressed

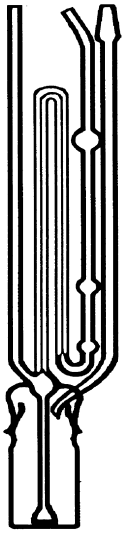

Figure 1 Off-line multi-bulb Bishop's capillary viscometer

samples were within the experimental uncertainty. Therefore, the d*n*/d*c* value was assumed equal to 0.150 ml g^{-1} for the HA samples both in 0.15 M NaCl and in 0.5 M NaCl solvents.

Viscometry. Intrinsic viscosity [η] of the UHMM HA samples was measured using a static off-line Bishop multi-bulb capillary viscometer. [η] of UHMM HA samples depends strongly on the shear rate. Hence, we have used a three-bulb capillary viscometer and the viscosity determined to three different shear rates was extrapolated to the zero-shear rate. The viscometer, *Figure 1*, consisted of three bulbs of 1.26, 0.67, 0.39 cm^3 volume and with a height 13.4, 7.1 and 2.2 cm (*h*) above the midpoint of each bulb. The inner diameter (*d*) and the length (*l*) of the capillary was, respectively, 0.5 mm and 32.4 cm. The apparent, not correct for non-newtonian flow, maximum shear rate ($\dot{\gamma}$) value was calculated according to the expression[4]:

$$\dot{\gamma} = \frac{\rho \cdot \boldsymbol{g} \cdot d \cdot h}{4 \cdot \eta_s \cdot \eta_r \cdot l} \tag{1}$$

were ρ is the density of the liquid, $\boldsymbol{g}$ is the acceleration of gravity and η_s the viscosity of the solvent. All the [η] measurements were carried out in 0.15 M NaCl solvent at 35°C.

Concentration of the samples. The concentration of the HA samples was measured by means of a capillary electrophoresis system. The analysis was carried out on a Beckman P/ACE 2200 instrument with UV detection at the wavelength of 200 nm. Capillary electrophoresis separation was performed on a fused silica capillary, 57 cm × 50 μm, from Applied Biosystem. HA separation was carried out in a pH 9 running buffer consisting of 50 mM sodium dodecyl sulphate, 50 mM sodium phosphate and 20 mM sodium tetraborate at 45°C. The applied voltage was 15 kV. Samples from fermentation were precipitated with ethanol and solubilized in 0.15 M NaCl solvent under agitation for 24 h. Concentration was calculated with respect to the area of a reference HA standard of known concentration.

Light scattering data-analysis

To obtain molar mass, dimension and second virial coefficient of the macromolecules the excess Rayleigh factor $R(\theta)$, with respect to the pure solvent, has to be measured over a wide range of concentrations and scattering angles. Using a MALS photometer the experiment consists of measuring the intensity of the scattering to some concentrations since the angular variation is measured simultaneously by means of the photodiodes array. From these data following the treatment of Zimm[5] the excess of Rayleigh factor for a monodisperse polymer may be expressed by the general equation:

$$R(\theta) = K \cdot (M \cdot P(\theta) \cdot c - 2A_2 \cdot M^2 \cdot P^2(\theta) \cdot c^2 + \ldots) \tag{2}$$

Taking the reciprocal of the previous equation leads to an equation which converges more rapidly[5]:

$$\frac{K \cdot c}{R(\theta)} = \frac{1}{M \cdot P(\theta)} + 2A_2 \cdot c + [3A_3 \cdot Q(\theta) - 4A_2^2 \cdot P(\theta) \cdot (1 - P(\theta))] \cdot c^2 + \ldots \tag{3}$$

where K is the optical constant, $K = (2\pi^2 n_0^2 (\mathrm{d}n/\mathrm{d}c)^2)/(\lambda_0^4 N_A)$, n_0 is the refractive index of the solvent, d*n*/d*c* is the specific refractive index increment, λ_0 is the wavelength of the light *in vacuo*, N_A is Avogadro's number, c is the concentration of the sample, θ is the angle between the detector and the incident primary light, M is the molar mass, A_2 and A_3 are the second and third virial coefficients, $P(\theta)$ is the particle scattering factor and $Q(\theta)$ is the scattering factor including the multiple interference effect. In the limit $\theta \rightarrow 0°$, both $P(\theta)$ and $Q(\theta) \rightarrow 1$. Generally, in the previous equations, the expansion of the series has stopped at the first order term. As a rule, the experimental results are expressed as a reduced Rayleigh factor: $K \bullet c/R(\theta)$. Then, the experimental data can be easily converted into the $P(\theta)$ function: $P(\theta) = [R(\theta)/R(0)]_{c=0} = [K \bullet c/R(0)]_{c=0}/[K \bullet c/R(\theta)]_{c=0}$.

In the MALS data analysis the commercial Dawn 3.01 software[6], from Wyatt, uses three formalisms labelled as 'Zimm', 'Debye' and 'Berry'. The formalisms labelled as 'Zimm' and 'Debye' use, respectively, equations (4) and (5). In the 'Berry' formalism the left-hand side of equation (4) is replaced with a square root. Obviously, equations (4) and (5), in the limit of very low concentrations, correspond respectively to equations (3) and (2). The root-mean-square radius $\langle s^2 \rangle^{1/2}$ and the A_2 values are obtained in the usual mode from the initial slope of the reduced $R(\theta)$ with respect to $\sin^2(\theta/2)$ and with respect to the concentration. It is well known that with polydisperse samples we obtain the weight-average molar mass M_w and the *z*-average root mean square radius $\langle s^2 \rangle_z^{1/2}$, in short hereafter referred to as the gyration radius (R_g).

$$\frac{K \cdot c}{R(\theta)} = \frac{1}{M \cdot P(\theta)} + 2A_2 \cdot c \tag{4}$$

$$\frac{R(\theta)}{K \cdot c} = M \cdot P(\theta) - 2A_2 M^2 P^2(\theta) \cdot c \tag{5}$$

Estimation of R_g for UHMM macromolecules requires more detailed comments. As usual, R_g has to be estimated from the initial slope of the $P(\theta)$ *versus* $\sin^2(\theta/2)$ plot. Unfortunately, the extrapolation for UHMM HA macromolecules is not simple. When R_g is sufficiently large, the $P(\theta)$ *versus* $\sin^2(\theta/2)$ plot shows noticeable curvature. In presence of curvature it is very difficult to estimate the initial slope. Further, Guinier[7] and Debye[8] showed that the $P(\theta)$ could be expressed independent of the shape and of the conformation of the macromolecules, in the limit $\mu^2 \bullet R_g^2/3 \ll 1$, as

follows:

$$P(\theta) = 1 - \frac{1}{3}\cdot\mu^2\cdot R_g^2 \tag{6}$$

where $\mu = 4\pi/\lambda\bullet\sin(\theta/2)$ and $\lambda = \lambda_0/n_o$ is the wavelength of the light in the medium. For UHMM HA macromolecules, considering that in our experimental condition the smallest accessible scattering angle was 14.5°, the Guinier equation was not valid. More exactly, the number of the detectors that could be used, in the Guinier region, to estimate the initial slope becomes very limited. Using the Guinier method it is very difficult to obtain a reliable estimate of the true R_g value for UHMM HA macromolecules. Considering these difficulties encountered in the extrapolation to zero angle of the $P(\theta)$ *versus* $\sin^2(\theta/2)$ plot for UHMM HA polymers we have chosen to fit the $P(\theta)$ experimental function with the classical Debye's equation[8]:

$$P(\theta) = \frac{2}{x^2}\cdot(e^{-x} - 1 + x) \tag{7}$$

where $x = \mu\bullet R_g$. Debye's equation is valid only for linear monodisperse random coils in an ideal θ-condition in which a Gaussian statistic could be assumed. To take account of the excluded volume effect in a good solvent we have used the Ptitsyn[9] and Hyde *et al.*[10] approach. This approach states that $P(\theta)$ could be expressed in the form:

$$P(\theta) = 2\cdot\int_0^1 1 - y\cdot\exp(-xy^{1+\epsilon})dy \tag{8}$$

Of course, for $\epsilon = 0$, equation (8), hereafter referred to as

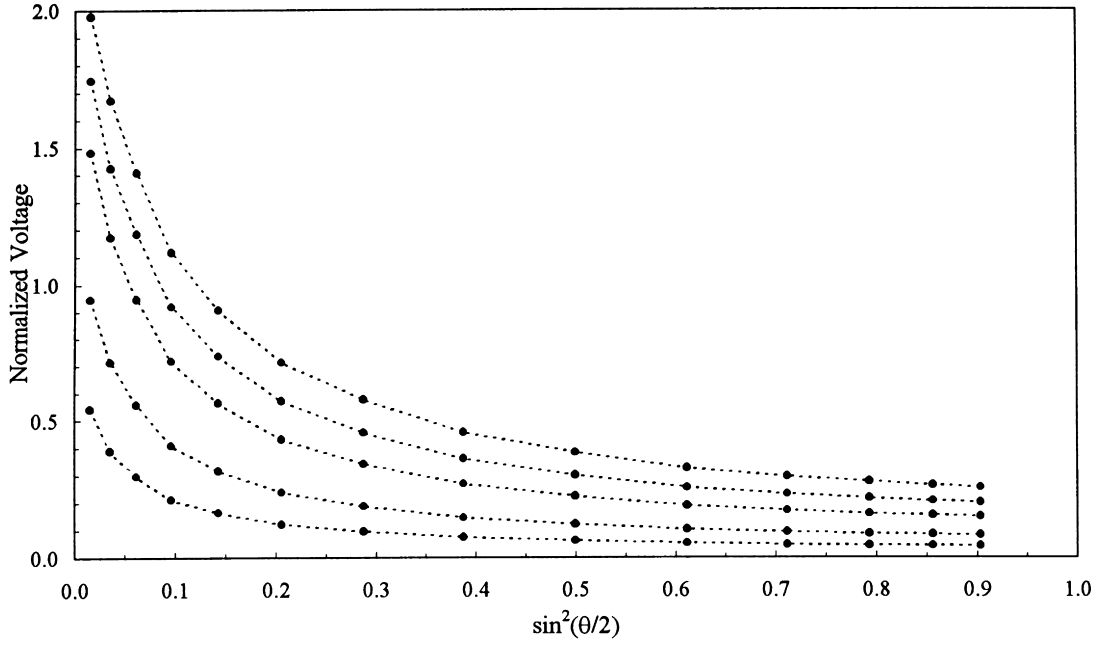

Figure 2 Scattering intensity of a UHMM HA sample ($M_w = 7.4 \times 10^6$); concentration from 1×10^{-5} to 6×10^{-5} g ml^{-1}

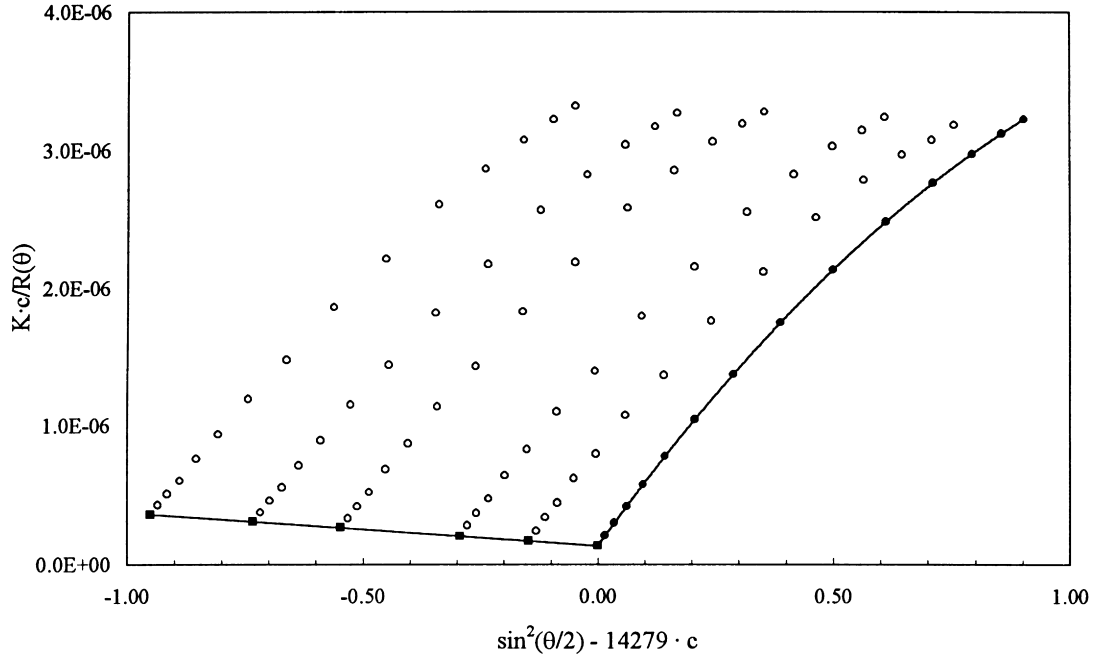

Figure 3 Zimm plot of a UHMM HA sample: equation Zimm, $c = 1°$, $\theta = 2°$

Ptitsyn's equation, reduces to Debye's equation. In equation (8), $P(\theta)$ depends on two adjustable parameters: R_g and ϵ. From the best fit between the experimental data and the theoretical Ptitsyn's equation it is possible to estimate the R_g value for UHMM HA samples.

RESULTS AND DISCUSSION

The characterization of HA as a consequence of its relevant interest and of its peculiar properties has attracted the attention of many researchers as attested by the volume of publications that have issued over the last 40 years[11–22]. Despite this significant interest, relevant data on the molecular characterization of UHMM HA polymers do not exist.

Static off-line MALS

Figure 2 shows the scattering intensity of a UHMM HA sample ($M_w = 7.4 \times 10^6$ g mol^{-1}). The concentration of the five solutions was very low, from 1×10^{-5} to 6×10^{-5} g ml^{-1}. The figure shows the unusual strong angular variation of the scattering. *Figure 3* shows the relative Zimm plot. In this case, we have used the 'Zimm' formalism, equation (4), and the data, in first approximation, are fitted with a 2° order polynomial for the angular variation, θ ranges from 14.5° to 151.3°, and a 1° order polynomial for the concentration. The results ($M_w = 7.4 \times 10^6$ g mol^{-1}, $R_g = 385.0$ nm, $A_2 = 1.66 \times 10^{-3}$ mol ml^{-1} g^{-2}) require an accurate evaluation. The extrapolation to infinite dilution does not present problems. *Figure 4* shows the $K \cdot c/R(\theta)$

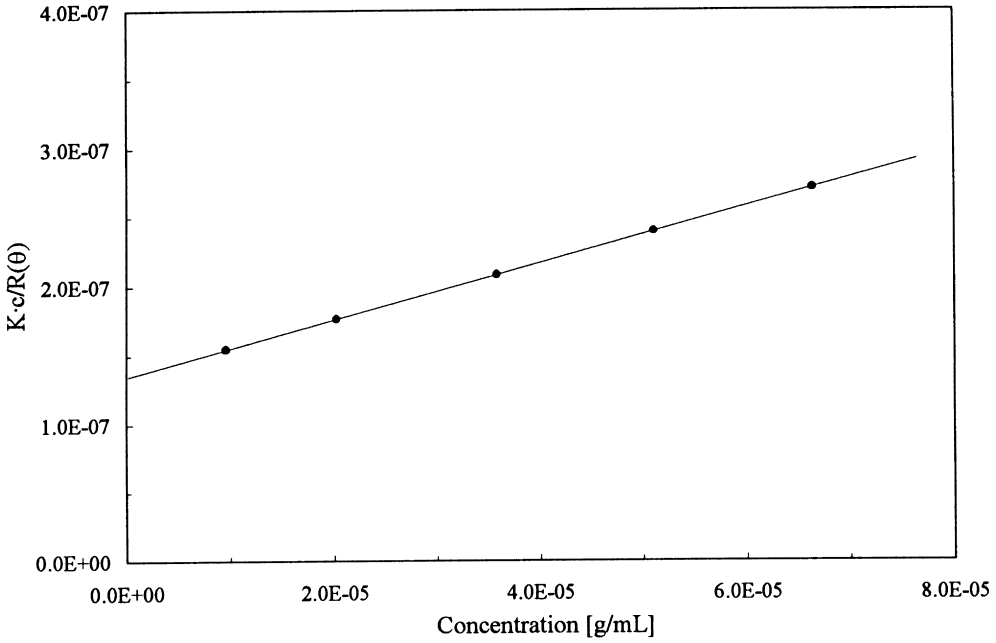

Figure 4 $K \cdot c/R(\theta)$ *versus* c plot: $M_w = 1.01 \times 10^7$ g mol^{-1}; c from 1×10^{-5} to 6.5×10^{-5} g ml^{-1}

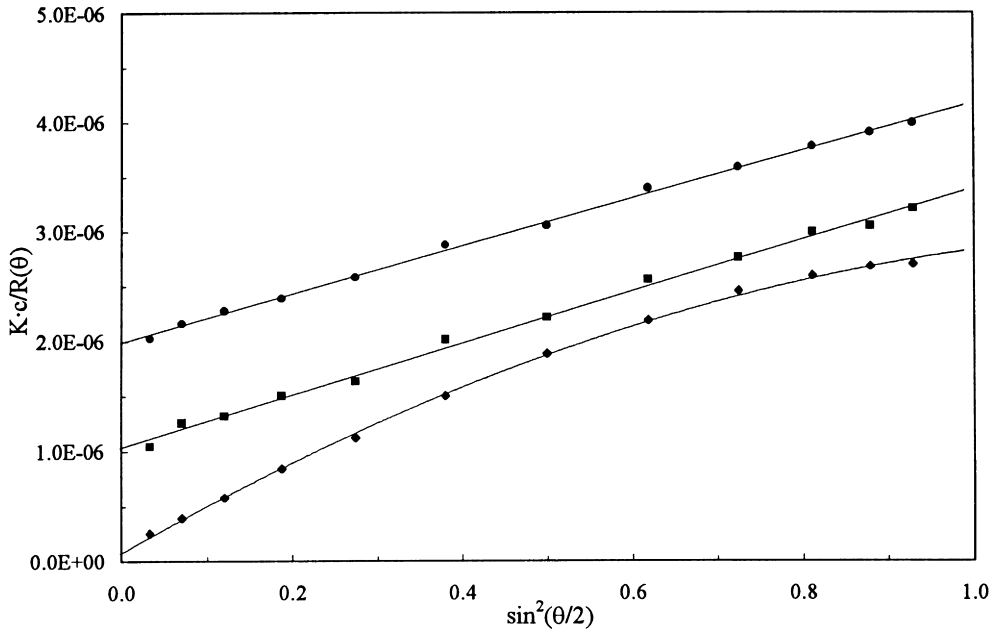

Figure 5 $K \cdot c/R(\theta)$ *versus* $\sin^2(\theta/2)$ plot for three UHMM HA samples: (●) $M = 5 \times 10^5$; (■) $M = 1.0 \times 10^6$; (♦) $M = 1.0 \times 10^7$

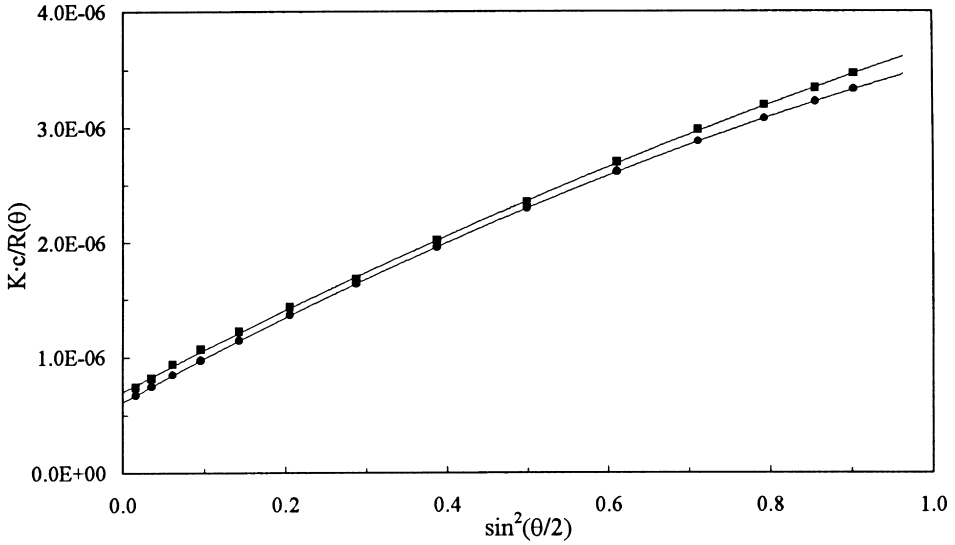

Figure 6 $K{\cdot}c/R(\theta)$ *versus* $\sin^2(\theta/2)$ plot for a UHMM HA sample from two methods: (●) MALS; (■) SEC-MALS

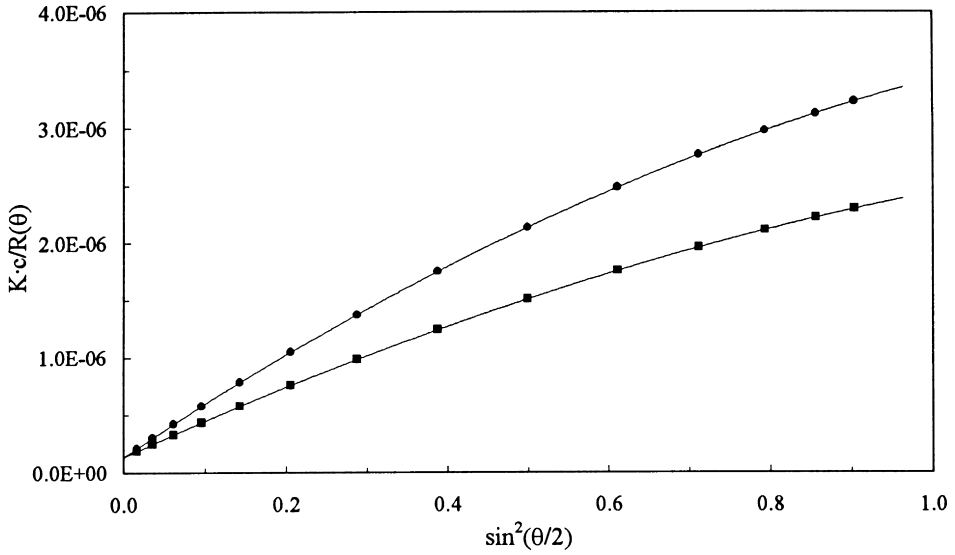

Figure 7 $K{\cdot}c/R(\theta)$ *versus* $\sin^2(\theta/2)$ plot for a UHMM HA sample in two solvents of different ionic strength: (●) 0.15 M NaCl; (■) 0.5 M NaCl

versus c plot for a sample with $M_w = 1.01 \times 10^7$ g mol^{-1} and c that ranges from 1×10^{-5} to 5×10^{-5} g ml^{-1}. The plot is linear, in the used range of concentration, also for this UHMM sample.

Figure 5 shows the $K{\bullet}c/R(\theta)$ *versus* $\sin^2(\theta/2)$ plot for three HA samples. The molar mass of the samples was, respectively, 5×10^5, 1×10^6 and 1×10^7 g mol^{-1}. The angular variation of the scattering is approximately linear up to 1×10^6 molar mass. When the molar mass of sample is greater than 1×10^6 the angular dependence of the scattering shows a noticeable downward curvature. As mentioned before, in the presence of a marked curvature the extrapolation to zero angle presents many problems[23,24]. The origins of the curvature could be various: polydispersity, excluded volume effect, stiffness of the chain. The dispersity of our HA samples was not high, it ranged from 1.5 to 1.8. *Figure 6* shows the $K{\bullet}c/R(\theta)$ *versus* $\sin^2(\theta/2)$ plot for an UHMM HA sample both from the off-line MALS method and from the on-line SEC-MALS method. Supposing ideal SEC fractionation, the SEC-MALS slices could be considered monodisperse in molar mass. There is not a notable difference on the curvature of the plot on the basis of the dispersity of our samples. *Figure 7* shows the influence on the curvature of the ionic strength of the solvent: 0.15 M NaCl against 0.5 M NaCl. In this case, the difference is evident and we could conclude that the curvature depends primarily from the excluded volume effect. Hence, in the extrapolation to zero angle we have chosen to use the Ptitsyn's equation.

Figure 8 shows the $K{\bullet}c/R(\theta)$ *versus* $\sin^2(\theta/2)$ plot for a UHMM HA sample, $M_w = 7.4 \times 10^6$ g mol^{-1}, in 0.5 M NaCl. The experimental data are well fitted by the Ptitsyn equation with $R_g = 312$ nm and the excluded volume effect parameter $\epsilon = 0.20$. For comparison, *Figure 8* also shows the $K{\bullet}c/R(\theta)$ *versus* $\sin^2(\theta/2)$ plot for linear random coils in ideal θ-condition and for infinitely thin rods. *Figure 9* shows the intercept and initial slope of the $K{\bullet}c/R(\theta)$ *versus* $\sin^2(\theta/2)$ plot estimated by three methods. The first is a linear fit using only the first five detectors (θ from 14.5° to 44.4°); the second is a 2° order polynomial fit using the first 12 detectors (θ from 14.5° to 125.6°); the third is the best fit using the Ptitsyn's equation for $P(\theta)$ and varying the values

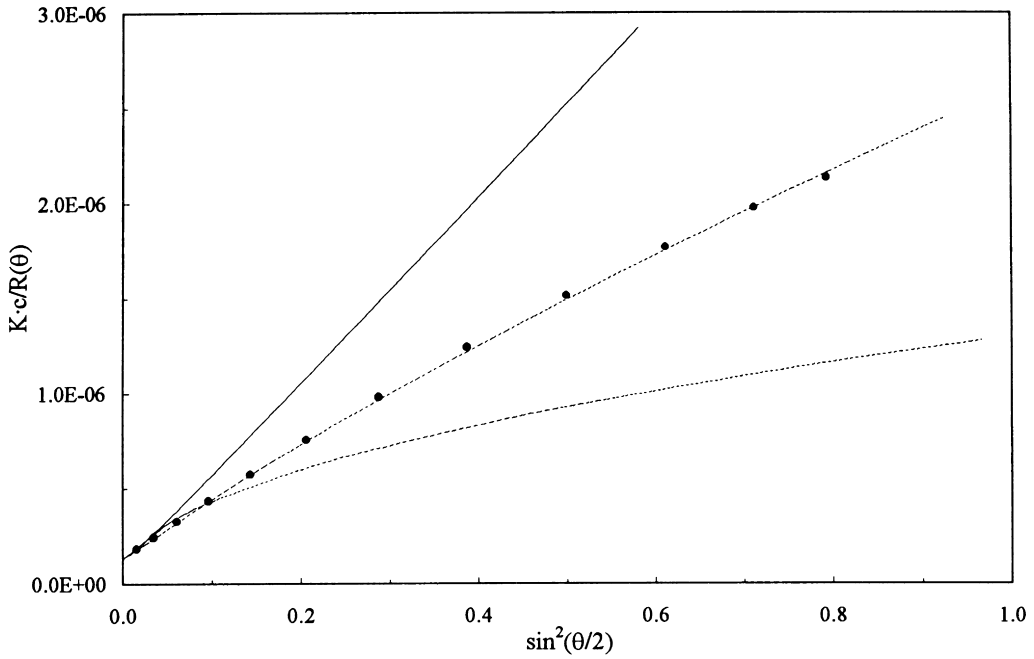

Figure 8 *K·c/R(θ) versus* $\sin^2(\theta/2)$ plot for a UHMM HA sample: (●) experimental; (——) coils in θ-condition; (– – –) coils with excluded volume, $\epsilon = 0.2$; (· · ·) rods

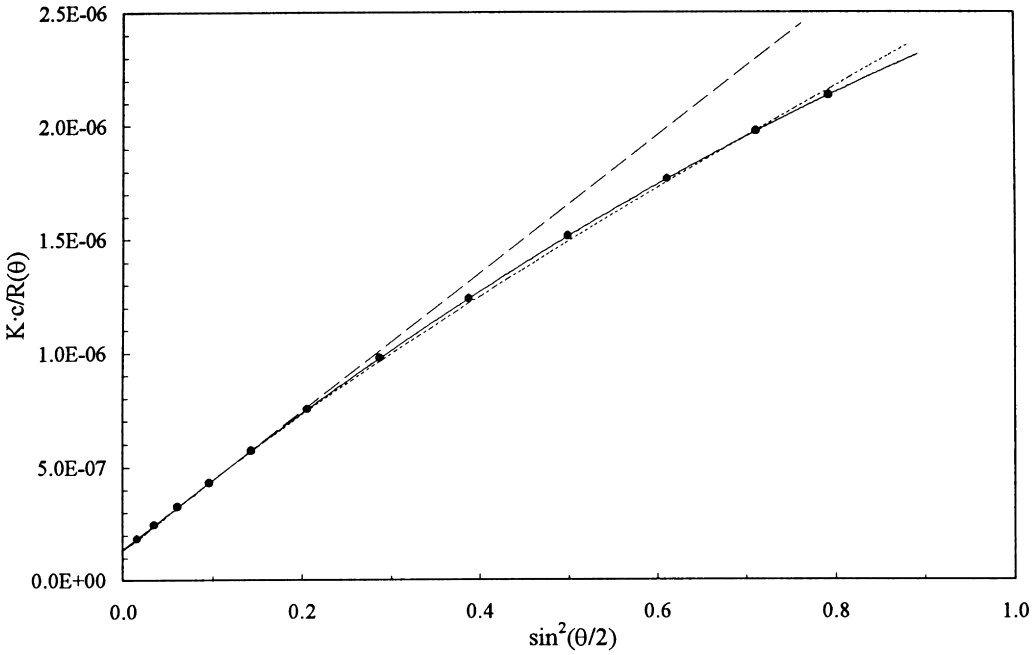

Figure 9 *K·c/R(θ) versus* $\sin^2(\theta/2)$ plot: (●) experimental; (– – –) linear fit for first five detectors; (——) polynomial 2° order fit; (· · ·) Ptitsyn's equation

of the adjustable parameters R_g and ϵ. *Table 1* shows the results, M_w and R_g, obtained using these three methods. Regarding the M_w values, there is a substantial agreement among the three methods. However, for R_g values there is a substantial agreement only between the 2° order polynomial and the Ptitsyn method. In the following, for convenience, the reported results have been obtained with the polynomial method. Obviously, our finding does not assume general meaning. We only state that in our specific case a second order polynomial fitting in the angular extrapolation to zero angle furnishes reliable M_w and R_g results.

Table 2 reports a summary of the results obtained in the characterization of 10 UHMM HA samples by means of static off-line MALS both in 0.15 M NaCl and in 0.5 M NaCl solvents. *Table 3* reports a comparison between M_w results obtained by MALS and LALS instruments. The agreement is very good and the differences were lower than 2.8%. LALS instrument measures the Rayleigh factor at very low angle, approximately 4–6°, and barely need extrapolation to zero angle. The agreement between MALS and LALS M_w data confirms that the extrapolation method, at least for the intercept, was correct.

A thorough examination requires the formalisms used in the MALS commercial software Dawn 3.01. When M_w and R_g values are not ultra-high the differences among the three formalisms 'Zimm', 'Debye' and 'Berry' are minimal. In

Table 1 Comparison between three elaboration methods: linear fit using the first five detectors, θ from 14.5° to 44.4°; polynomial 2° order fit using 12 detectors, θ from 14.5° to 125.6°; best fit using the Ptitsyn's equation

Sample	Solvent	Linear		Polynomial		Ptitsyn		ϵ
		$M_w \times 10^{-6}$	R_g (nm)	$M_w \times 10^{-6}$	R_g (nm)	$M_w \times 10^{-6}$	R_g (nm)	
HA09	0.15 M NaCl	7.34	371.2	7.40	385.0	7.39	391.0	0.22
HA09	0.5 M NaCl	7.32	309.2	7.35	320.4	7.32	318.0	0.20

Table 2 Summarized results for UHMM HA samples by off-line MALS in 0.15 M NaCl and 0.5 M NaCl solvents

Sample	0.15 M NaCl			0.5 M NaCl	
	$M_w \times 10^{-6}$ (g mol^{-1})	R_g (nm)	$A_2 \times 10^3$ (mol ml^{-1} g^{-2})	R_g (nm)	$A_2 \times 10^3$ (mol ml^{-1} g^{-2})
HA01	1.06	125.7	1.86	110.0	1.07
HA02	1.65	163.4	1.81	147.4	1.03
HA03	3.31	247.4	1.80	213.7	0.96
HA04	3.50	257.7	1.81	221.7	0.98
HA05	5.00	300.3	1.76	263.2	0.96
HA06	5.40	328.6	1.72	276.9	0.93
HA07	6.98	368.3	1.71		
HA08	7.27	383.5	1.64		
HA09	7.40	385.0	1.66	320.4	0.92
HA10	10.01	461.5	1.64		

Table 3 Comparison between MALS and LALS M_w results

Sample	MALS $M_w \times 10^{-6}$	LALS $M_w \times 10^{-6}$	Difference (%)
HA04	3.5	3.6	−2.8
HA05	5.0	5.0	0.0
HA06	5.4	5.5	−1.8
HA09	7.4	7.6	−2.6

Table 4 Intrinsic viscosity characterization of two UHMM HA samples

Sample	$[\eta]$ (dl g^{-1})	$M_v \times 10^{-6}$ (g mol^{-1})	$M_w \times 10^{-6}$ (g mol^{-1})
HA10	26.64	2.33	2.60
HA11	50.37	6.73	7.40

the UHMM polymers, characterization of the differences are important. It is worth noting that it is very important to measure the scattering angle as low as possible. Using a K5 flow cell in 0.15 M NaCl solvent the smallest measurable angle was 14.5°. Berry[25] suggests using the $[K \bullet c/(R(\theta)]^{1/2}$ *versus* $\sin^2(\theta/2)$ plot in the presence of non linear scattering angular variation. Wyatt[3] suggests using the 'Debye' formalism, equation (5), for UHMM polymers. In our specific case it was impossible to fit the angular scattering variation using the 'Debye' or the 'Berry' formalisms[2].

$\langle s^2 \rangle^{1/2} = f(M)$ *power law*. Using the data listed in the *Table 2* we obtain the following slopes of the $\langle s^2 \rangle^{1/2}$ *versus* molar mass power law ($\langle s^2 \rangle^{1/2} = K \bullet M^{\alpha}$): $\alpha = 0.569$ in 0.15 M NaCl solvent and $\alpha = 0.547$ in 0.5 M NaCl solvent. *Figure 10* shows the relative $\langle s^2 \rangle^{1/2} = f(M)$ power laws for HA in these solvents. The slopes are in significant agreement with the results reported by Fouissac *et al.*[20] for HA polymers in different ionic strength. The congruence between M_w and R_g data allows us to state that our method of elaboration of the MALS data, particularly the method of evaluation of gyration radius values, furnishes reliable and congruent results.

Second virial coefficient A_2. Data of the second virial coefficient are listed in the *Table 2*. The results are in significant agreement with the A_2 data reported in the literature[12–17] for HA polymers in aqueous solvent of similar ionic strength. It is worth noting the high positive value of A_2 and the relatively low dependence, in the explored range, with respect to the molar mass.

Off-line viscometry

The usual average shear rate (1500–2000 s^{-1}) of an Ubbelohde viscometer is too high for non-newtonian solutions such as UHMM HA polymers. Only with a double extrapolation, shear-rate and concentration, is it possible to get a correct non-apparent value of $[\eta]$. Using our viscometer, the apparent shear rate values for the three bulbs, calculated with the equation (1), were approximately: 600, 300 and 90 s^{-1}. The $[\eta]$ value has remained calculated by means of Huggins, $(\eta_{sp}/c)_o = f(c)$, and Kraemer, $(\ln(\eta_r)/c)_o = f(c)$, equations using the zero shear rate reduced, $(\eta_{sp}/c)_o$, and inherent, $(\ln(\eta_r)/c)_o$, viscosity. *Figure 11* shows the shear rate dependence of η_{sp}/c for two UHMM HA samples. Molar mass of the two sample was quite different. M_w and concentration of the two HA samples were, respectively: 2.6×10^6 g mol^{-1}, 5.1×10^{-3} g dl^{-1} and 7.4×10^6 g mol^{-1}, 4.2×10^{-3} g dl^{-1}.

Table 4 reports the obtained intrinsic viscosity value for the two HA samples previous described. *Figure 12* shows the intrinsic viscosity plot, Huggins' equation, for the higher molar mass sample. The intrinsic viscosity of the sample, 50.37 dl g^{-1}, was very high. In *Table 4* we also report the viscosity-average molar mass M_v calculated from the $[\eta]$ values by means of the Mark–Houwink–Sakurada equation using the constants ($k = 3.97 \times 10^{-3}$ dl g^{-1}, $a = 0.601$) obtained from the literature[18] for high molar

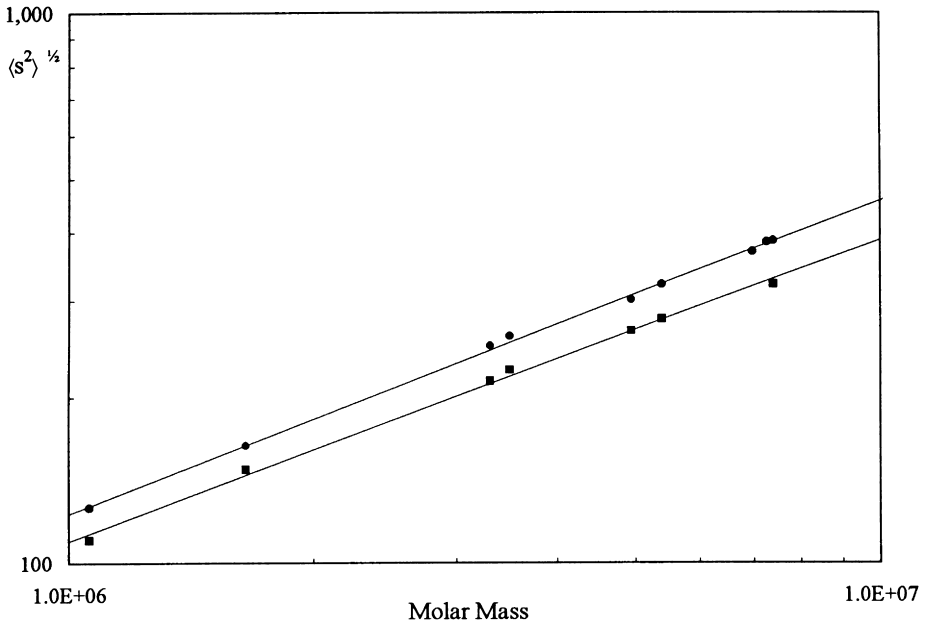

Figure 10 $\langle s^2 \rangle^{1/2} = f(M)$ power law: (●) 0.15 M NaCl; (■) 0.5 M NaCl

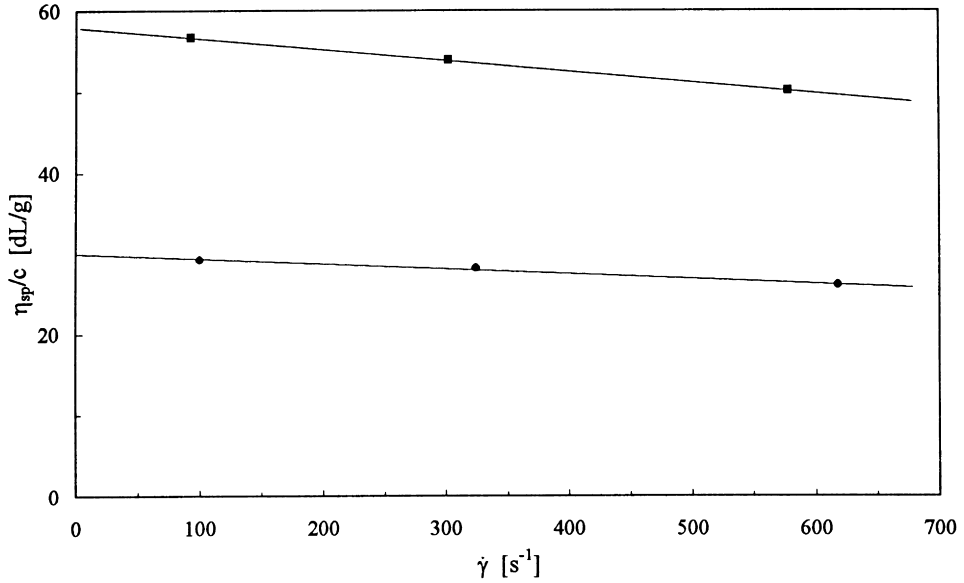

Figure 11 Shear rate dependence of η_{sp}/c for two UHMM HA samples: (●) $M_w = 2.6 \times 10^6$ g mol^{-1}; (■) $M_w = 7.4 \times 10^6$ g mol^{-1}

mass ($M > 1 \times 10^6$ g mol^{-1}) HA polymers. The calculated M_v value is consistent with the M_w value obtained from off-line MALS.

Persistence length

From the dependence of the gyration radius on the molar mass, the stiffness of the HA chain can be estimated. The stiffness of the HA chain can be estimated by the persistence length of the polymer. A convenient method to estimate the persistence length, one half of the Kuhn's statistical segment λ^{-1}, of HA as a function of the ionic strength was described by Fouissac *et al.*[20]. Fouissac builds upon the model of Odijk[26]. In Odijk's model the total persistence length L_t of a wormlike polyelectrolyte chain can be expressed as:

$$L_t = L_p + L_e \tag{9}$$

where L_p is the intrinsic persistence length of the polymer and L_e is the contribution of the electrostatic repulsion to the total persistence length. The gyration radius of the macromolecules as a function of the molar mass or of the contour length (L) of the macromolecules, $L = M/M_L$, can be expressed as:

$$\langle s^2 \rangle = \frac{1}{3} \cdot L \cdot L_t \cdot \alpha_{s,el}^2 \tag{10}$$

where $\alpha_{s,el}$ is the electrostatic expansion factor with respect to the ideal condition and M_L is the mass per unit length. A detailed and complete description of the method can be found in the original papers[20,26] and will not reported herein. Assuming[27] $M_L = 410$ nm^{-1} and $L_t = L_p$ for higher ionic strength data, 0.5 M NaCl, where the electrostatic contribution to L_t is almost screened out, we obtain a persistence length value of 9.8 nm. *Figure 13* shows the

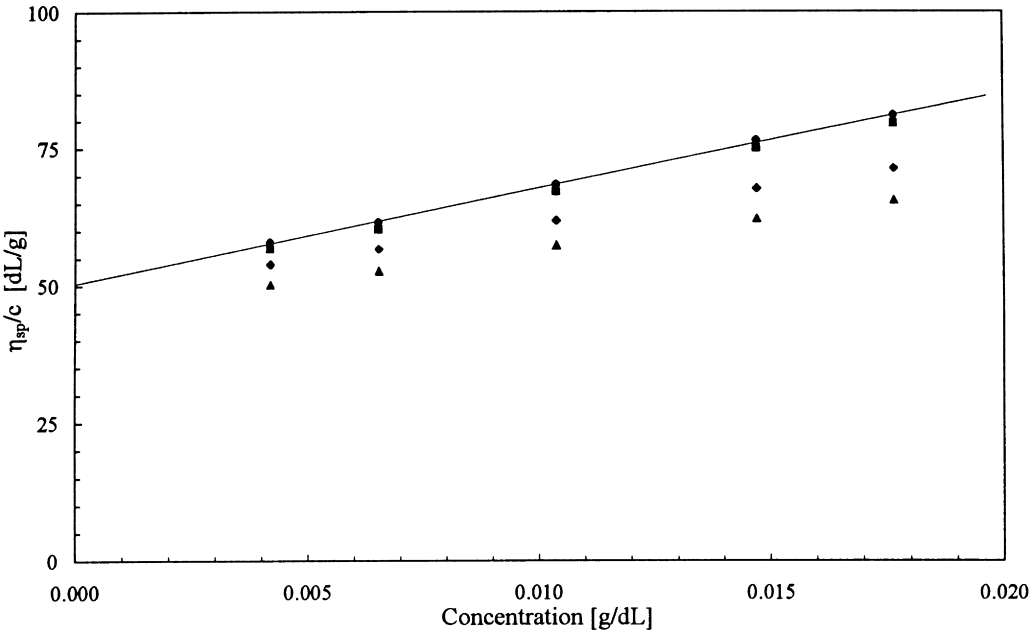

Figure 12 Zero-shear rate [η] for a UHMM HA sample: from top to bottom (●) $\dot{\gamma} = 0\ s^{-1}$; (■) $\dot{\gamma} \approx 90\ s^{-1}$; (◇) $\dot{\gamma} \approx 300\ s^{-1}$; (▲) $\dot{\gamma} \approx 600\ s^{-1}$

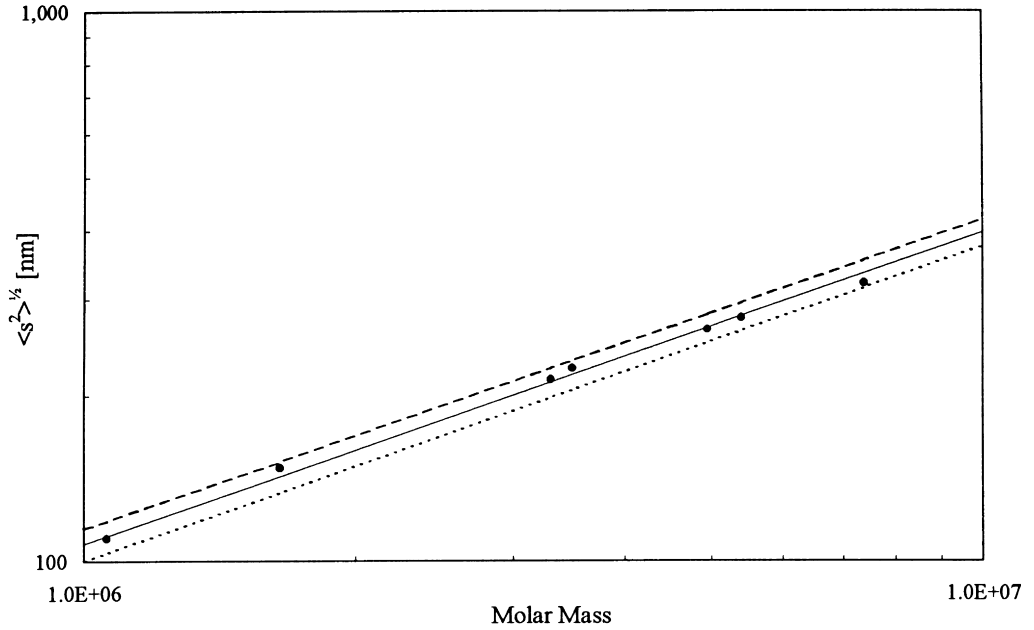

Figure 13 $\langle s^2 \rangle^{1/2} = f(M)$ power law for HA polymer: (●) experimental; calculated: (···) $L_t = 8$ nm; (——) $L_t = 10$ nm; (– – –) $L_t = 12$ nm

$\langle s^2 \rangle^{1/2} = f(M)$, experimental and calculated, power laws in 0.5 M NaCl solvent. In such a figure we can see the good agreement between experimental and calculated values, equation (10), when $L_t = 10$ nm.

Alternatively, the persistence length may be derived using a modified Stockmayer–Fixman method[28] for random coil macromolecules in a good solvent. In such a method, $(\langle s^2 \rangle_z / Mz)^{3/2}$ is plotted as function of $Mz^{1/2}$ and extrapolated to zero molar mass. Such a plot is shown in *Figure 14*. For HA polymer in 0.5 M NaCl solvent this analysis produces a persistence length of 9.5 nm that is very close to that obtained using the previous method. In this analysis we have assumed $m_o = 189\ g\ mol^{-1}$, $l_o = 0.519$ nm and $\Phi = 2.5 \times 10^{21}$: where m_o is the average molar mass of a monosaccharide of HA, l_o is the average intersaccharide distance and Φ is Flory's constant[19].

A persistence length value of 9.5–9.8 nm is a little higher than the value, 8.5 nm, obtained by Fouissac *et al*. in 0.3 M NaCl. Values of the HA persistence length in the literature range from 2 to 20 nm[19,27], and in some cases are more than 20 nm. Choosing the data obtained in similar conditions we get an average value of the persistence length that ranges from 8 to 14 nm. Our persistence length value is in good agreement with these average values. Therefore, we can conclude that our molar mass and gyration radius data for UHMM polymers produce a congruent estimation of the stiffness of the HA chain. Again, this result is another indirect confirmation that the elaboration method of the MALS data was largely correct.

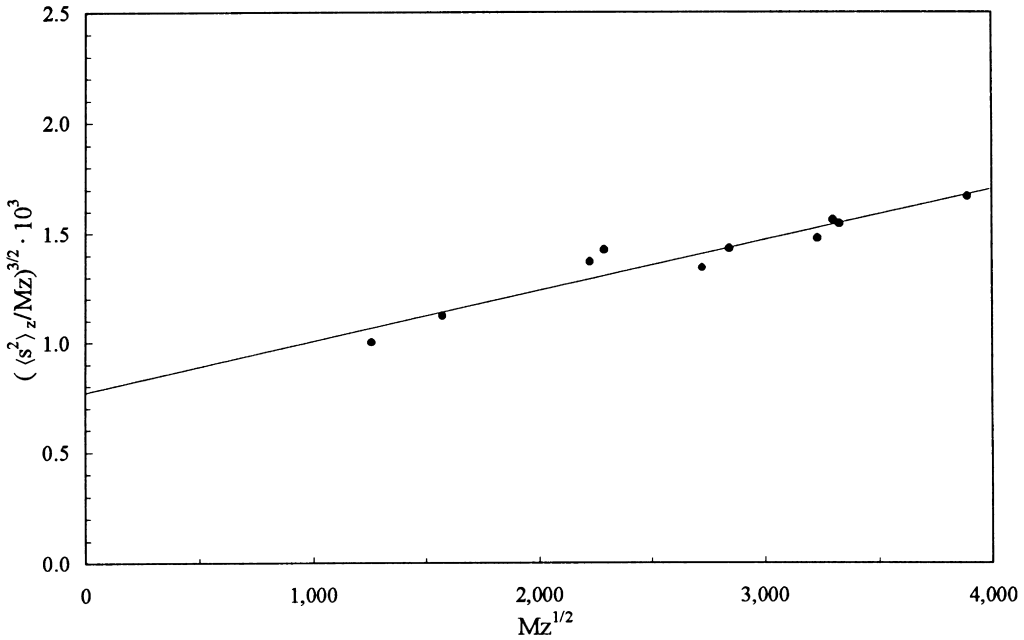

Figure 14 Persistence length of HA polymer calculated by a modified Stockmayer–Fixman's plot: $(\langle s^2\rangle_z/Mz)^{3/2}$ *versus* $Mz^{1/2}$

CONCLUSIONS

A successful characterization of UHMM HA polymers requires optimization of the experimental protocol and verification of the data-analysis algorithms. The critical point in the characterization of UHMM HA is the fractionation in the SEC columns. Therefore, a preliminary characterization by means of static off-line MALS and off-line viscometry methods was carried out. MALS characterization of UHMM HA presents the problem of non linear angular variation of the scattering. We have presented a method to obtain reliable M_w and R_g results in the presence of notable curvature. The intrinsic viscosity characterization requires a double extrapolation, concentration and shear rate, to obtain a correct non apparent value of $[\eta]$. Despite these difficulties, this study shows that it is possible to successfully characterize UHMM HA polymers with a molar mass up to 1×10^7 g mol^{-1}. The static off-line methods that we have used in this study are cumbersome and a little unsuitable for the quality control of the HA samples, but produce reliable M_w, R_g and $[\eta]$ results.

ACKNOWLEDGEMENTS

The authors thank Geofrey Taylor, Pharmacia & Upjohn, who purified all the HA samples from the fermentative source.

REFERENCES

1. Nguyen, T. Q. and Kausch, H. H., *Proc. Int. GPC Symp.*, San Francisco, CA, 1991, p. 373.
2. Mendichi, R. and Giacometti Schieroni, A., *Proc. Int. GPC Symp.*, San Diego, CA, 1996, p. 183.
3. Wyatt, P. J., *Analyt. Chim. Acta*, 1993, **272**, 1.
4. Einaga, Y., Miyaki, Y. and Fujita, H., *J. Polym. Sci. Polym. Phys.*, 1979, **17**, 2103.
5. Zimm, B. H., *J. Chem. Phys.*, 1948, **16**, 1093.
6. Wyatt Technology Corporation, Dawn 3.01 Manual Software, A.5, 1993.
7. Guinier, A., *Ann. Phys.*, 1939, **12**, 161.
8. Debye, P., *J. Phys. Colloid Chem.*, 1947, **51**, 18.
9. Ptitsyn, O. B., *Zhur Fiz. Chim.*, 1977, **31**, 1091.
10. Hyde, A. J., Ryan, J. H., Wall, F. T. and Schatzki, T. F., *J. Polym. Sci.*, 1958, **33**, 129.
11. Laurent, T. C. and Gergely, J., *J. Biol. Chem.*, 1955, **212**, 325.
12. Cleland, R. L. and Wang, J. L., *Biopolymers*, 1970, **9**, 799.
13. Cleland, R. L., *Biopolymers*, 1970, **9**, 811.
14. Cleland, R. L., *Arch. Biochem. Biophys.*, 1977, **180**, 57.
15. Ribitsch, G., Schurz, J. and Ribitsch, V., *Colloid Polym. Sci.*, 1980, **258**, 1322.
16. Cleland, R. L., *Biopolymers*, 1984, **23**, 647.
17. Ueno, Y., Tanaka, Y., Horie, K. and Tokuyasu, K., *Chem. Pharm. Bull.*, 1988, **36**, 4971.
18. Bothner, H., Waaler, T. and Wik, O., *Int. J. Biol. Macromol.*, 1988, **10**, 287.
19. Ghosh, S., Reed, C. E. and Reed, W. F., *Biopolymers*, 1990, **30**, 1101.
20. Fouissac, E., Milas, M., Rinaudo, M. and Borsali, R., *Macromolecules*, 1992, **25**, 5613.
21. Fouissac, E., Milas, M. and Rinaudo, M., *Macromolecules*, 1993, **26**, 6945.
22. Soltes, L., Mislovicova, D. and Sebille, B., *Biomed. Chromatogr.*, 1996, **10**, 53.
23. Mijnlieff, P. F. and Coumou, D. J., *J. Colloid Interface Sci.*, 1968, **27**, 553.
24. Fujita, H., *Polym. J.*, 1970, **1**, 537.
25. Berry, G. C., *J. Chem. Phys.*, 1966, **44**, 4550.
26. Odijk, K. and Houwaart, A. C., *J. Polym. Sci. Polym. Phys.*, 1978, **16**, 627.
27. Gamini, A., Paoletti, S. and Zanetti, F., *Laser Light Scattering in Biochemistry*, Royal Society of Chemistry, Cambridge, 1992.
28. Bauman, H., *J. Polym. Sci. Polym. Lett.*, 1965, **3**, 1069.